HHS Public Access

Author manuscript

Neuroimaging Clin N Am. Author manuscript; available in PMC 2016 August 26.

Published in final edited form as:

Neuroimaging Clin N Am. 2009 November ; 19(4): 657–668. doi:10.1016/j.nic.2009.08.014.

Brain irradiation: Effects on normal brain parenchyma and radiation injury

Pia C Sundgren, M.D., Ph.D. and

Diagnostic Centre for Imaging and Functional Medicine, Malmö University Hospital, University of Lund, SE-205 02 Malmö, Sweden

Yue Cao, Ph.D.

Radiation Oncology, University of Michigan and Radiology, Ann Arbor, Michigan 48109-0010, USA. Phone: +1 734-647-2914, Fax: +1 734 - 936-2261, yuecao@umich.edu

SYNOPSIS

In this chapter, the clinical and neurobehavioral symptoms and signs of radiation-induced brain injury, possible histopathology, and the potential of functional, metabolic and molecular imaging as a biomarker for assessment and prediction of neurotoxicity after brain irradiation and imaging findings in radiation necrosis will be discussed.

Keywords

irradiation; radiation injury; neurotoxicity; diffusion tensor imaging; magnetic resonance imaging; magnetic resonance spectroscopy

INTRODUCTION

Radiation therapy (RT) is a major treatment modality for malignant and benign brain tumors. However, concerns of radiation effects on the brain tissue and neurcognitive function as well as quality of life increase as survival of the patients treated for brain tumors is improving. Radiation effects on the brain manifest as late neurological sequelae and neurocognitive dysfunction with or without gross tissue necrosis (1-4). Late neurocognitive dysfunction presents as diminishing mental capacity for working memory, learning ability, executive function, and attention. Recent multi-center studies of patients with low-grade gliomas who are without clinical signs of tumor recurrence after radiation treatment show that both a high total dose as well as a high dose per fraction are associated with neurocognitive deterioration, especially memory functions (4,5). Radiation-induced functional, metabolic and molecular changes in the brain structures and neural networks, which can be assessed by in vivo imaging, could be responsible for neurocognitive function changes.

Corresponding author: Pia C Sundgren, MD., PhD phone: +46-40-338990, Fax: +46 40 338798, pia.sundgren@med.lu.se.

In this review, we discuss clinical and neurobehavioral symptoms and signs of radiation-induced brain injury, possible histopathology, and the potential of functional, metabolic and molecular imaging as a biomarker for assessment and prediction of neurotoxicity after brain irradiation and imaging findings in radiation necrosis.

CLINICAL, RADIOLOGICAL AND NEUROBEHAVIORAL SYMPTOMS AND SIGNS

Clinical symptoms and signs

Classically, clinical complications after brain therapeutic irradiation have been described as acute (days to weeks after irradiation), subacute or early delayed (2-6 months after the completion of RT), and late effects (6 months to years after the completion of RT) (1,6,7).

The *acute reaction* to conventional fractionated brain irradiation is usually mild, characterized by headache, nausea, drowsiness, and sometimes worsening of neurological symptoms. Corticosteroids are usually successful in relieving acute complications.

Reports on *early delayed reactions* increase with frequency following contemporary cranial irradiation techniques. General neurological deterioration during this interval (2-6 months after RT) is believed to be secondary to transient, diffuse demyelination. Many focal neurologic signs following radiation treatment of intracranial tumor have been attributed to intralesional reactions, probably indicative of tumor response and/or perilesional reactions (i.e., edema or demyelination). However, periventricular white matter (WM) lesions start to appear on conventional MRI or CT during this interval even with standard fractionated partial brain RT (8,9). Following high-dose, volume-limited stereotactic radiosurgery (SRS), transient WM alterations are often apparent on conventional MRI, generally beginning 6 or more months after treatment (10,11). Following high dose, large brain-volume treatment and concurrent chemotherapy, necrosis, particularly in WM, starts to develop in this interval, and the location of necrosis is often near the site of the original tumor (12,13).

The classical *late effect* following brain irradiation is either localized or multi-focal necrosis, often associated with high dose and large brain-volume treatment (7,12-14). Complications include worsening neurological signs/symptoms, seizures, and increased intracranial pressure. Nevertheless, WM abnormality is a much more common late effect, and is often noted extending peripherally beyond the high-dose volume following partial brain irradiation (8,9). WM abnormality as well as necrosis is progressive (8-11) and their imaging findings will be discussed later.

Neurological symptoms and neurocognitive impairments related to WM injury range from mild personality change to progressive memory loss, and to marked, incapacitating dementia (15).

Radiological signs

The radiological signatures of WM alterations have been categorized as (1) periventricular changes, (2) focal extension of intense signal into WM; (3) diffuse extension into WM; and

(4) diffuse coalescence of white and gray matter into intense signal region, loss of architecture, cortical atrophy, and hydrocephalus(8).

Following focal or whole brain irradiation asymptomatic focal edema is a commonly finding seen both on CT and MR typically presenting as increased signal on T2-weighted and FLAIR images in the white matter on MRI (Fig 1) and as decreased attenuation in the white matter on CT.

Radiation necrosis is often difficult to differentiate from recurrent tumor as the imaging pattern is very similar and they have many shared characteristics such as it origin that often is at or in the vicinity of the original tumor and they often demonstrate heterogeneous contrast enhancement. Commonly radiation necrosis presents as a single focal enhancing lesion but it can be multifocal, or even in the contralateral side. The side may vary and range from small nodular enhancement to large areas necrosis and heterogeneous enhancement (16). Most of lesions consist of an enhancing mass with a central area of necrosis often in a so called soap-bubble or Swiss-cheese pattern (13) (Fig 2). On T2-weighted images, the solid portion of the radiation-induced necrotic mass has low signal intensity, and the central necrotic component shows increased signal intensity (13).

In the milder forms of radiation induced injury the pattern of enhancement can be nodular, linear or curvilinear and present in as single or multiple lesions of varying sizes. Commonly the lesion growth over time, demonstrates surrounding edema, and causes mass effect. Typical locations for radiation necrosis is in the postsurgical tumor bed, in the periventricular white matter especially corpus callosum and centrum semiovale (on top of the ventricles) because the periventricular white matter is very s susceptible to radiation. Radiation injury and radiation necrosis can occur outside the high-dose radiation dose field (16) (Fig 3).

Neurobehavioral symptoms and signs

In recent years, many efforts have been focused on *late neurocognitive dysfunction* and *quality of life* of patients with brain tumors and treated by RT with or without concurrent chemotherapy. Although a few studies find that the deterioration of neurocognitive function is an indicator of tumor progression (17,18), a recent multi-center study of patients with low-grade gliomas who had no clinical signs of tumor recurrence at least one year after treatment showed that a high total dose correlated with a decline in working memory and that a high dose per fraction interfered with long-term memory storage and retrieval [4]. Also, in a randomized trial of low- (50.4 Gy) versus high-dose (64.8 Gy) RT in patients with supratentorial low-grade glioma, significant cognitive deterioration from baseline was found in those without tumor progression, with rates of 8.2%, 4.6%, and 5.3% at years of 1, 2, and 5 respectively, as assessed by the relatively insensitive Folstein Mini-Mental State Examination (MMSE) (5). Moreover, the rate of cognitive impairment is even higher using a battery of neuropsychological tests, which are much more sensitive to cognitive functions than the MMSE (4,15,19,20). Also, neurocognitive dysfunction is observed without radiation necrosis (15), consistent with the findings in an animal study (21).

The cognitive domains of these dysfunctions present primarily in memory function, learning ability and executive function, and to a lesser extent in fine motor skills and attention.

The potential effect of RT on neurocognitive outcomes is an important factor in the determination of the risks versus benefits of treatment (22), which should be an integral part of clinical decision-making. Given the late nature of neurocognitive dysfunction, it would be important to identify in vivo imaging biomarkers for early assessment and prediction of late neurotoxicity.

HISTOPATHOLOGY IN RADIATION-INDUCED BRAIN INJURY

Radiation-induced injury in cerebral tissue is a highly complex and interactive process involving multiple tissue elements (2,23,24). Cerebral vascular injury has long been recognized to occur acutely and precedes subacute demyelination and reactive astrocytic and microglial responses (25-28). Histopathologic studies reveal that lifting of endothelia from the basement membrane, dilation and thickening of blood vessels, endothelial cell nuclear enlargement, and hypertrophy of perivascular astrocytes are among the first effects after irradiation (29-31). Early endothelial cell death and apoptosis after irradiation have been detected (26,27,32). Possible mechanisms of endothelial apoptosis include generation of intracellular ceramide via acidic sphingomyelinase and adhering leukocytes via TNF-α (27,32,33). The initial injury of vessels is followed by the formation of platelet matrix and thrombi, which eventually results in occlusion and thrombosis in microvessels within weeks to months (23,34). Furthermore, cerebral vascular injury is followed by degenerative structural changes in WM (29-31,35). The lag time between vascular injury and WM degeneration depends upon the severity of the injury. Together, these observations strongly support the concept that cerebral vascular injury is of crucial importance for the development of WM injury following irradiation.

In addition to vascular abnormalities, demyelination is another typical histopathology of radiation-induced brain tissue injury. It has been shown that irradiation results in the loss of reproductive capacity of the oligodendrocyte type 2 astrocyte (O-2A) progenitor cells in both brain and spinal cord of adult rats (36-38). Presumably, radiation-induced loss of O-2A progenitor cells results in failure to replace normal turned-over oligodendrocytes, with the eventuall consequence of demyelination. However, the kinetics of oligodendrocyte loss is inconsistent with the late onset of necrosis.

The brain is a highly integrated system, comprising a number of disparate phenotypes of cells. Thus, brain irradiation could affect not only vasculature and O-2A progenitors, but also astrocytes, microglia, neurons, and recently identified neural stem cells (39). As suggested, the response of neural tissue to irradiation also involves oxygen stress, inflammatory response, secondary reactive processes and enhanced cytokine gene expression (2,23,24). To date, our understanding of histopathology and molecular biology after brain response to irradiation is limited.

RADIATION NECROSIS AND PSEUDO-PROGRESSION

The differentiation of recurrent tumor or progressive tumor from radiation injury after radiotherapy is often a radiological dilemma regardless the technique used - CT or MR. Most of these brain neoplasms have been subjected to radiation and/or chemotherapy and many of the tumors do not have specific imaging characteristics that will enable the neuroradiologist to discriminate tumor recurrence from the inflammatory or necrotic change that can result from treatment with radiation and/or chemotherapy. Both entities typically demonstrate contrast enhancement. It is, therefore, often the clinical course, a brain biopsy, or imaging over a lengthy follow-up interval that enable the distinction of recurrent tumor from a treatment-related lesion and not the specific imaging itself (13).

While the difficulties in differentiation between radiation necrosis and a recurrent tumor often occur several months after the initial therapy recent studies have described transient increases in contrast enhancement immediately after chemo-radiation which mimic tumor progression and has been termed “pseudo-progression” (40-44).

The incidence of pseudo-progression following concurrent chemo-radiation has been reported to occur in approximately 15-30% of patients (40-44). The majority of patients remained clinically stable despite imaging changes suggestive of tumor progression. Radiation-induced vascular changes leading to focal transient increase in gadolinium enhancement following irradiation has been considered a possible mechanism (40). The combination of chemotherapy and radiation therapy may increase the incidence of pseudo-progression, possibly due to the increased radiosensitive effect of temozolomide on adjacent normal tissue (41-44). Pseudo progression is further discussed in the Chapter Therapeutic Advances in Malignant Glioma: Current Status and Future Prospects.

IMAGING AS A BIOMARKER FOR RADIATION-INDUCED NEURO-TOXICITY AND RADIATION NECROSIS

Today, a large body of converging evidence, from histopathology, molecular biology, animal models and clinical observations, suggests that radiation-induced neurotoxicity follows an interactive and dynamic sequence as early vascular injury, subsequent focal and diffuse demyelination, late tissue degeneration and neurocognitive dysfunction. Although limited, functional and metabolic imaging has been utilized to investigate vascular injury, WM demyelination, and metabolic change in cerebral tissue after irradiation without apparent tissue necrosis. The functional and metabolic changes have been associated with radiation dose, dose volume, and fraction size. Furthermore, a few studies have attempted to link the functional and metabolic changes in the brain to neurocognitive function changes.

In the following sections, we will review the studies of white matter injury and radiation necrosis using diffusion tensor imaging, and changes in cerebral blood flow, blood volume and metabolism using functional MRI, proton spectroscopy, and PET. Changes in cerebral blood flow, blood volume in the work-up to distinguish radiation necrosis from recurrent brain tumor will be discussed in the chapter MR Perfusion and Permeability in Brain Tumor.

Diffusion tensor imaging

Diffusion tensor imaging (DTI) is the most sensitive technique to assess WM integrity and histopathological changes before structural changes are visible on any other imaging modalities. DTI is able to assess water diffusion as well as anisotropic diffusion in the tissue structures (45-47). In WM, the tight myelin sheaths surrounding the axon substantially restrict water diffusion in the direction perpendicular to the axon axis ($\lambda_{\perp}$) compared to water diffusion in the direction along the axon axis ($\lambda_{\parallel}$). Therefore, anisotropic water diffusion can be used to characterize tissue types, e.g., grey matter (GM) and WM, and to provide information on the density and orientation of WM fiber tracts. Furthermore, the quantitative indices obtained from DTI can aid in distinguishing between myelin loss and axonal injury. For example, an increase in $\lambda_{\perp}$ with or without a change in $\lambda_{\parallel}$ has been confirmed to be an *in vivo* biomarker for demyelination with pathology in myelin-deficient rats (48). In a recent study of radiation-induced white matter damage in a rodent model, an early delayed increase in $\lambda_{\perp}$ after irradiation was correlated with demyelination histologically while a decrease in $\lambda_{\parallel}$ was correlated with reactive astrogliosis without necrosis (49). Either $\lambda_{\perp}$ increase or $\lambda_{\parallel}$ decrease can lead to fractional anisotropy (FA) decreases.

Diffusion tensor imaging has been used to assess white matter injury in the pediatric and adult patients treated with brain radiation. In a recent study of children with medulloblastoma treated with craniospinal irradiation, decreased FA in WM after radiation was found to be correlated inversely with the age at treatment and positively with craniospinal dose (50). In a cross-sectional study of survivors of childhood medulloblastoma and acute lymphoblastic leukemia treated with craniospinal irradiation, differences of WM FA in the patients and in age-matched control group had a significant effect on intelligence quotient (IQ) scores after adjusting effects of age at treatment, craniospinal dose, and time interval since treatment (51). In another study of the survivors of acute lymphoblastic leukemia 17-37 years after craniospinal irradiation, FA was analyzed in the temporal lobe, hippocampus, and thalamus, and found to be reduced compared to aged matched control [52]. However, since neurocognitive functions in these patients were not evaluated, and neurobehavioral consequences of degradation of these functional structures are unknown. Although findings from these cross-sectional studies identify several interesting factors that might contribute to radiation-induced neurocognitive injury in the pediatric population, future prospective studies are required to test hypotheses generated from these preliminary investigations.

In the adult patients who undergo partial or whole brain radiation therapy, several prospective studies showed changes in DTI indices of normal appearing white matter (53,54). In a study of 25 patients who had high-grade glioma, low-grade glioma or benign tumors and underwent partial brain RT, progressive decreases in FA from the start of RT to 45 weeks after were observed in large WM fibers of the genu and splenium of corpus callosum (53). Also, the decrease in FA was dose-dependent. Further analysis showed progressive increases in $\lambda_{\perp}$ but little change in $\lambda_{\parallel}$, suggesting demyelination predominant after WM irradiation. In another study of 26 patients who underwent prophylactic cranial irradiation, decreases in FA of several WM anatomic sites, including frontal white matter,

corona radiate and cerebellum, were observed at the end of RT, and six weeks after RT, the extent of which appears to depend upon risk factors of vascular diseases (54). Whether the radiation-induced WM injury is structural selective is question that remains to be answered. Also, how these observed WM changes are associated with neurocognitive function changes remains to be tested.

Recent studies utilizing diffusion weighted imaging (DWI) to differentiate recurrent tumor from radiation injury (55) have shown that the apparent diffusion coefficient (ADC) ratios in the contrast-enhancing lesion are lower in recurrent tumor than in radiation induced injury [55]; however other investigators using diffusion tensor imaging (DTI) (56) demonstrated significantly higher ADC values in the contrast enhancing part of the lesion in patients with tumor recurrence than in the contrast enhancing lesion in patients with radiation injury. That study also showed that the ADC ratios in the white matter tracts in the peri-lesion oedema were significantly higher in radiation injury patients compared with those with recurrent tumor and that the FA ratios were significantly higher in normal appearing white matter tracts adjacent to the oedema in patients diagnosed with radiation injury compared to those with recurrent tumours (56). Both $\lambda_{\parallel}$ and $\lambda_{\perp}$ values were significantly higher in contrast-enhancing lesions in patients with recurrent tumor than in those with radiation injury (P=.02) as well as in the perilesional edema for both patient groups compared with normal appearing white matter. It can be anticipated that higher ADC values found in areas of tumor recurrence could be due to increased extracellular space and micronecrosis, as commonly found in brain tumors, although a high-cell-density tumor would exhibit low ADC. Lower ADC value in radiation injury could be a result of gliosis, fibrosis, macrophage invasion, vascular changes and demyelination. These radiation-induced effects will restrict water mobility (lower ADC) relative to simple non-cellular or cystic necrosis, which elevates ADC. Contradictory, are results from another study that demonstrated higher ADC values in treatment-related changes/radiation necrosis than in solid tumors, suggesting that solid tumors may have more densely packed cells than necrotic tissues, resulting in a lower ADC for recurrent tumor (57). It have been suggested, supported by data both from animal and human studies, that diffusion imaging may be sensitive for evaluating early tumor response to therapy [58,59] suggesting that early increase in ADC values during therapy may relate to therapy-induced cell necrosis. The subsequent drop in tumor ADC to pretreatment levels could be an indicator of tumor regrowth (58,59).

Proton spectroscopy

Magnetic resonance spectroscopy (MRS) is a non-invasive technique for measurement of chemical substances (metabolites) in the brain and may serve as a sensitive imaging tool to non-invasively detect neurochemical changes as evidence of neurotoxicity in the irradiated brain (60-68) The technique has been used to differentiate recurrent tumor from radiation necrosis (69-71) while only a few prospective studies evaluating interval changes in metabolic activity in normal appearing brain parenchyma during and following cranial RT for primary brain neoplasm have been published (63-68,72).

The most common technique have been single voxel 1H-MRS technique with only a limited part of the brain evaluated and only at one or two time points during and after irradiation

(63-65,72), less frequent has two-dimensional (2D) multivoxel spectroscopy (66,68) or three-dimensional (3D) spectroscopic imaging (67) been used for interval follow-up during or after radiation therapy.

It have been hypothesized that structural degradation in cerebral tissue after radiation therapy would be predicted by early changes in metabolic activity detectable by MRS before the development of neurocognitive symptoms or anatomic changes seen on conventional MRI. This hypothesis is supported by the findings in a recent study of 11 adult patients with either low-grade glioma or benign tumors without previous cranial irradiation (68). That study demonstrated significant alterations in brain metabolites occurred in normal-appearing human brain parenchyma early during radiation treatment and that interval progression of some of these changes occurred over at least a 6 month period (68). This was especially evident by the interval decrease in N-acetylaspartate/ creatine (NAA/Cr) and choline/ creatine (Cho/Cr) ratios from the pre treatment values at 3 weeks of radiation treatment and the progressive decline seen in the ratios at 6 months after the completion of radiation treatment (68) (Fig 4). The conclusion from that study was that the decrease in the NAA/Cr ratio is most likely due to neuronal damage, neuronal cell death due to apoptosis, and neuronal dysfunction secondary to the irradiation. The metabolite NAA is predominantly present in neurons and believed to represent a marker of neuronal density and function and creatine is a marker of energy metabolism and is considered to be fairly stable under most conditions. The presumption that NAA decreases following radiation is also supported by other previous studies demonstrating a decrease in whole brain NAA and in the NAA concentration of irradiated brain (62-64,72). Observations of decreases in both choline and choline compounds, as well as the decreased Cho/Cr ratio have also been reported after irradiation (60,67,68,73). The choline compound is correlated with cell membrane biosynthesis and metabolic turnover in proliferative tissue and it has been suggested that the decrease in Cho seen in normal appearing brain tissue after irradiation might be due to membrane damage in the myelin or the myelin-producing oligodendrocytes, accompanied by impaired tissue perfusion (74). One of the few previous reports of metabolic changes after prophylactic irradiation, in patients with acute lymphoblastic leukemia (60) found that the lower NAA/Cr and Cho/Cr was associated with the presence of hemosiderin but not with imaging findings of leukoencephalopathy.

Also recent animal studies have demonstrated significant differences in brain metabolite concentrations in irradiated rat brain (75) accompanied by worsening on behavioral tests in the irradiated rats compared to sham-irradiated rats 54 weeks after radiation treatment (76).

Specific spectroscopic changes that occur in radiation necrosis have been reported and include slight depression of NAA and variable changes in Cho and Cr (71, 77-79). In addition, radiation necrosis may show a broad peak between 0 and 2 ppm, probably reflecting cellular debris containing fatty acids, lactate and amino acids (80) (Fig 5). Also other metabolites have been suggested to be present in radiation necrosis. For example in one study monitoring the progression of severe cerebral radiation injuries in the temporal lobes in patients previously treated for nasopharyngeal carcinoma a unknown resonance named Px in the 2.37–2.40 ppm region was found in affected temopral lobes. The authors

speculated if Px could be associated with anaerobic glycolysis producing pyruvate (2.37 ppm) or succinate (2.40 ppm) as can be seen in brain abscess formations (81).

Overall it looks like higher Cho/NAA and Cho/Cr ratios are to be expected in areas of recurrent tumor compared to areas of radiation injury as well as to normal adjacent brain tissue as reported by several studies. Different MRS studies using different spectroscopy technique have reproted an 80-97% success rate to retrospectively differentiate recurrent tumour from radiation injury with significantly increased Cho/NAA and Cho/Cr ratios (69,70, 79).

Different so called metabolic cut off values have been suggested differentiate recurrent tumour from radiation injury (69). A previous study utilizing 2D CSI reported that when cut-off values of 1.8 for either Cho/NAA or Cho/Cr were used - i.e. values above 1.8 being diagnostic for tumor recurrence - 27 out of 28 patients were retrospectively correctly diagnosed (69). Values that are in agreement with those in a previous study utilizing multivoxel ^{1}H-MRSI and correlation with histological specimens (70) in which the investigators claim that a Cho/Cr ratio over 1.79 or Lip-lac/Cho ratio less then 0.75 has a 7-fold increased odds of being pure tumor compared to pure necrosis and the odds of the biopsy's being pure necrosis and having either the Cho/nCr values less than 0.89 or a Cho/nCho value less than 0.66 are six times the odds of the biopsy's being pure tumor (70). Another study using receiver operating characteristic analysis reported the sensitivity, specificity and diagnostic accuracy of 3D 1H-MRS to be 94.1%, 100%, and 96.2%, respectively, based on the cut-off values of 1.71 for Cho/Cr or 1.71 for Cho/NAA or both as tumor criterion (82). The Choline/lipid or lactate ratio (Cho/(Lip or Lac)) is another ratio that has been used in the attempt to diagnose radiation necrosis is the Cho/(Lip or Lac) ratio. In another study the authors reported positive predictive values of a Cho/Lip or Lac ratio less than 0.3 and the positive predictive values of a Cho/Cr ratio less than 2.48 for diagnosing radiation necrosis were 100% and 71.4%, respectively. (83).

However we have to bare in mind that many of these newly occurring do not only consist of large areas of pure tumor or radiation injury/necrosis but rather is a mixture of tumor cells and tissue with radiation injury is present. This assumption is supported by a prior study of multivoxel MRS that found that: “spectral patterns do allow reliable differential diagnostic statements to be made when the tissues are composed of either pure tumor or pure necrosis, but the spectral patterns are less definitive when tissues composed of varying degrees of mixed tumor and necrosis are examined” (84).

Positron Emission Tomography - PET

Previous PET studies have shown that areas of radiation injury have lower glucose metabolism than normal brain tissue because they have lower cellular density (85). A previous PET review reports the sensitivity of PET to be 80-90% and the specificity to be 50-90% in differentiating late-delayed radiation injury from recurrent high grade glioma (86). Another study of 15 patients with histopathologically confirmed diagnosis reported that FDG-PET was only 43% sensitive in distinguishing recurrent tumor from radiation effect, and was least accurate when the lesion volume was less than 6 cc (87). However, false

positive FDG-PET and Tl-201 SPECT have been reported with biopsy proven radiation necrosis (88).

FDG-PET and ^{15}O-PET (cerebral blood flow) have been used to relate dose-dependent radiolgocial defined changes innnormal brain tissue to neurocognitive dysfunction. In that recent study a dose-dependent response of CNS tissue was detected using FDG-PET and the decrease in CNS metabolism correlated with decreased performance on neuropsychological tests (89). They also demonstrated transient changes in cerebral blood flow with ^{15}O; increased relative cerebral blood flow with increasing dose measured by an increase in ^{15}O changes at 3 weeks after treatment in areas receiving greater then 30 Gy by significantly lower levels at 6 months after treatment (89).

^{11}C-Methonine PET (Met-PET) have in a few recent studies demonstrated the possiblity to accurately distinguish recurrent brain tumor from radiation necrosis. In a recent MET-PET study of 21 patients previously treated for primary or secondary neoplasm presenting with a total of 27 lesions the authors report intense MET uptake in patients with recurrent tumor (mean 1.79±0.32 vs 1.05±0.11, $p<0.0001$) while no significant MRT uptake were seen patients with radiation necrosis with 100% sensitivity, specificity and accuracy of visual interpretation of the MET uptake (90).

More about the use of PET imaging to differentiate radiation necrosis from recurrent tumor will be discussed in the Chapter Molecular imaging (PET) of brain tumors.

Vascular imaging

There are limited reports about the cerebral blood flow (CBF) and cerebral blood volume (CBV) changes in normal brain that has be irradiated. The limited existing reports indicate that there are changes in the CBF and CBV after irradiation and that these changes might be dose-dependent (89, 91-94).

In a prospective study of DCE MRI of prediction of radiation-induced neurocognitive dysfunction (92) Cao et al found that vascular volumes and blood-brain barrier (BBB) permeability increased significantly in the high dose regions during RT, followed by a decrease after RT. Changes in both vascular volume and BBB permeability correlated with the doses accumulated at the time of scans at week 3 and 6 during RT and 1 month after RT. The effect of the dose-volume on the vascular volume was also observed. Finally, changes in verbal learning scores 6 months after RT were significantly correlated with changes in vascular volumes of left temporal and frontal lobes and changes in BBB permeability of left frontal lobes during RT. Similar correlation was found between recall scores and BBB permeability. These data suggest that the early changes in cerebral vasculature may predict delayed alterations in verbal learning and total recall, which are important components of neurocognitive function.

Mean and regional cerebral blood flow (CBF) was measured at before, 2 weeks and 3 months after stereotactic radiosurgery (SRS) in a 99mTc-HMPAO to elucidate the radiation effect on the normal brain after SRS (92). They found significant reductions in mean CBF

(by 7%) and regional CBF in the peri-target areas (by 5-7%) and out-of-field areas (by 6-22%) were recognized at 2 weeks and 3 months after SRS (93).

Another study using dynamic-susceptibility contrast perfusion MR imaging demonstrated lower relative CBV in normal appearing brain tissue 2 months after radiotherapy suggesting a dose-dependent decline in vessel density and increase in vascular permeability and/or tortuosity in irradiated normal-appearing brain tissue (91).

A recent study utilizing perfusion computed tomography demonstrated higher nCBV and nCBF and lower nMTT compared with radiation necrosis (94).

More about the use of perfusion imaging both with MR and CT to differentiate radiation necrosis from recurrent tumor will be discussed in the Chapter MR Perfusion and Permeability in Brain Tumor.

CONCLUSION

In conclusion, several different imaging techniques points in the same direction that occult injury to the normal brain occur during radiation treatment. In the future these different imaging biomakers might be able to compare the effects of different radiation treatment regimens and to evaluate neuroprotective therapies with the potential to minimize the neurotoxicity of brain radiation treatment.

The differentiation of recurrent tumor from radiation injury remains a challenge and the combination of conventional MR imaging and more than one of the other more advanced imaging modalities such as MRS and PET are often needed to come to a conclusion.

References

1. Schultheiss TE, Kun LE, Ang KK, et al. Radiation response of the central nervous system. Int J Radiat Oncol Biol Phys. 1995; 31:1093–112.
2. Tofilon PJ, Fike JR. The radioresponse of the central nervous system: a dynamic process. Radiat Res. 2000; 153:357–70.
3. Khuntia D, Brown P, Li J, et al. Whole-brain radiotherapy in the management of brain metastasis. J Clin Oncol. 2006; 24:1295–304.
4. Klein M, Heimans JJ, Aaronson NK, et al. Effect of radiotherapy and other treatment related factors on mid-term to long-term cognitive sequelae in low-grade gliomas: a comparative study. Lancet. 2002; 360:1361–8.
5. Brown PD, Buckner JC, O'Fallon JR, et al. Effects of radiotherapy on cognitive function in patients with low-grade glioma measured by the folstein mini-mental state examination. J Clin Oncol. 2003; 21:2519–24.
6. Hopewell JW, Wright EA. The nature of latent cerebral irradiation damage and its modification by hypertension. Br J Radiol. 1970; 43:161–7.
7. Sheline GE, Wara WM, Smith V. Therapeutic irradiation and brain injury. Int J Radiat Oncol Biol Phys. 1980; 6:1215–28.
8. Constine LS, Konski A, Ekholm S, et al. Adverse effects of brain irradiation correlated with MR and CT imaging. Int J Radiat Oncol Biol Phys. 1988; 15:319–30.
9. Tsuruda JS, Kortman KE, Bradley WG, et al. Radiation effects on cerebral white matter: MR evaluation. AJR Am J Roentgenol. 1987; 49:165–71.

10. Flickinger JC, Lunsford LD, Kondziolka D, et al. Radiosurgery and brain tolerance: an analysis of neurodiagnostic imaging changes after gamma knife radiosurgery for arteriovenous malformations. Int J Radiat Oncol Biol Phys. 1992; 23:19–26.
11. Loeffler JS, Siddon RL, Wen PY, et al. Stereotactic radiosurgery of the brain using a standard linear accelerator: a study of early and late effects. Radiother Oncol. 1990; 17:311–21.
12. Van Tassel P, Bruner JM, Maor MH, et al. MR of toxic effects of accelerated fractionation radiation therapy and carboplatin chemotherapy for malignant gliomas. AJNR Am J Neuroradiol. 1995; 16:715–26.
13. Kumar AJ, Leeds NE, Fuller GN, et al. Malignant gliomas: MR imaging spectrum of radiation therapy- and chemotherapy-induced necrosis of the brain after treatment. Radiology. 2000; 217:377–84.
14. Kramer S. Radiation effect and tolerance of the central nervous system. Front. Radiat. Ther. Oncol. 1972; 6:332–345.
15. Postma TJ, Klein M, Verstappen CC, et al. Radiotherapy-induced cerebral abnormalities in patients with low-grade glioma. Neurology. 2002; 59:121–3.
16. Sundgren, PC.; Elias, A.; Rogers, L., et al. Correlation of MR imaging morphologic abnormalities, MR spectroscopy, and radiation treatment dose volumes in histologically proved cerebral radiation necrosis.. Programs and abstracts of the 47th Annual meeting of the American Society of Neuroradiology.; Vancouver. 2009; p. 219-220.
17. Mehta MP, Shapiro WR, Glantz MJ, et al. Lead-in phase to randomized trial of motexafin gadolinium and whole-brain radiation for patients with brain metastases: centralized assessment of magnetic resonance imaging, neurocognitive, and neurologic end points. J Clin Oncol. 2002; 20:3445–53.
18. Meyers CA, Brown PD. Role and relevance of neurocognitive assessment in clinical trials of patients with CNS tumors. J Clin Oncol. 2006; 24:1305–9.
19. Roman DD, Sperduto PW. Neuropsychological effects of cranial radiation: current knowledge and future directions. Int J Radiat Oncol Biol Phys. 1995; 31:983–98.
20. Crossen JR, Garwood D, Glatstein E, et al. Neurobehavioral sequelae of cranial irradiation in adults: a review of radiation-induced encephalopathy. J Clin Oncol. 1994; 12:627–42.
21. Hodges H, Katzung N, Sowinski P, et al. Late behavioural and neuropathological effects of local brain irradiation in the rat. Behav Brain Res. 1998; 91:99–114.
22. Mulhern RK, Palmer SL, Merchant TE, et al. Neurocognitive consequences of risk-adapted therapy for childhood medulloblastoma. J Clin Oncol. 2005; 23:5511–9.
23. Belka C, Budach W, Kortmann RD, et al. Radiation induced CNS toxicity--molecular and cellular mechanisms. Br J Cancer. 2001; 85:1233–9.
24. Wong CS, Van der Kogel AJ. Mechanisms of radiation injury to the central nervous system: implications for neuroprotection. Mol Interv. 2004; 4:273–84.
25. Price RE, Langford LA, Jackson EF, et al. Radiation-induced morphologic changes in the rhesus monkey (Macaca mulatta) brain. J Med Primatol. 2001; 30:81–7.
26. Ljubimova NV, Levitman MK, Plotnikova ED, et al. Endothelial cell population dynamics in rat brain after local irradiation. Br J Radiol. 1991; 64:934–40.
27. Pena LA, Fuks Z, Kolesnick R. Radiation-induced apoptosis of endothelial cells in the murine central nervous system: protection by fibroblast growth factor and sphingomyelinase deficiency. Cancer Res. 2000; 60:321–7.
28. Li YQ, Chen P, Haimovitz-Friedman A, et al. Endothelial apoptosis initiates acute blood-brain barrier disruption after ionizing radiation. Cancer Res. 2003; 63:5950–6.
29. Calvo W, Hopewell JW, Reinhold HS, et al. Time- and dose-related changes in the white matter of the rat brain after single doses of X rays. Br J Radiol. 1988; 1:1043–52.
30. Reinhold HS, Calvo W, Hopewell JW, et al. Development of blood vessel-related radiation damage in the fimbria of the central nervous system. Int J Radiat Oncol Biol Phys. 1990; 8:37–42.
31. Okeda R, Okada S, Kawano A, et al. Neuropathology of delayed encephalopathy in cats induced by heavy-ion irradiation. J Radiat Res (Tokyo). 2003; 44:345–52.

32. Santana P, Pena LA, Haimovitz-Friedman A, et al. Acid sphingomyelinase-deficient human lymphoblasts and mice are defective in radiation-induced apoptosis. Cell. 1996; 86:189–99.
33. Eissner G, Kohlhuber F, Grell M, et al. Critical involvement of transmembrane tumor necrosis factor-alpha in endothelial programmed cell death mediated by ionizing radiation and bacterial endotoxin. Blood. 1995; 86:4184–93.
34. Verheij M, Dewit LG, Boomgaard MN, et al. Ionizing radiation enhances platelet adhesion to the extracellular matrix of human endothelial cells by an increase in the release of von Willebrand factor. Radiat Res. 1994; 137:202–7.
35. Fike JR, Sheline GE, Cann CE, et al. Radiation necrosis. Prog Exp Tumor Res. 1984; 28:136–51.
36. van der Maazen RW, Kleiboer BJ, Verhagen I, et al. Irradiation in vitro discriminates between different O-2A progenitor cell subpopulations in the perinatal central nervous system of rats. Radiat Res. 128:64–72. 19991.
37. van der Maazen RW, Kleiboer BJ, Verhagen I, et al. Repair capacity of adult rat glial progenitor cells determined by an in vitro clonogenic assay after in vitro or in vivo fractionated irradiation. Int J Radiat Biol. 1993; 63:661–6, 1993.
38. van der Maazen RW, Verhagen I, Kleiboer BJ, et al. Radiosensitivity of glial progenitor cells of the perinatal and adult rat optic nerve studied by an in vitro clonogenic assay. Radiother Oncol. 1991; 20:258–64.
39. Monje ML, Mizumatsu S, Fike JR, et al. Irradiation induces neural precursor-cell dysfunction. Nat Med. 2002; 8:955–62.
40. DeWit MC, de Bruin HG, Eijkenboom W, et al. Immediate post-radiotherapy changes in malignant glioma can mimic tumor progression. Neurology. 2004; 63(3):535–7.
41. Brandsma D, Stalphers L, Taal W, et al. Clinical features, mechanisms, and management of pseudoprogression in malignant gliomas. Lancet Oncology. 2008; 9(5):453–61.
42. Taal W, Brandsma D, de Bruin H, et al. Incidence of Early Pseudo-progression in a cohort of malignant glioma patients treated with chemoirradiation with temozolomide. Cancer. 2008; 113(2):405–410.
43. Brandes AA, Franceschi E, Tosoni A, et al. MGMT promoter methylation status can predict the incidence and outcome of pseudoprogression after concomitant radiochemotherapy in newly diagnosed glioblastoma patients. J Clin Oncol. 2008; 26(13):2192–7.
44. Gerstner ER, McNamara MB, Norden AD. Effect of adding temozolomide to radiation therapy on the incidence of pseudo-progression. J Neurooncol. Feb 17.2009 (epub).
45. Basser PJ, Pierpaoli C. Microstructural and physiological features of tissues elucidated by quantitative-diffusion-tensor MRI. J Magn Reson B. 1996; 111:209–19.
46. Basser PJ, Pierpaoli C. A simplified method to measure the diffusion tensor from seven MR images. Magn Reson Med. 1998; 39:928–34.
47. Pierpaoli C, Jezzard P, Basser PJ, et al. Diffusion tensor MR imaging of the human brain. Radiology. 1996; 201:637–48.
48. Song SK, Sun SW, Ramsbottom MJ, et al. Dysmyelination revealed through MRI as increased radial (but unchanged axial) diffusion of water. Neuroimage. 2002; 17:1429–36.
49. Wang S, Wu EX, Qiu D, et al. Longitudinal diffusion tensor magnetic resonance imaging study of radiation-induced white matter damage in a rat model. Cancer Res. 2009; 69:1190–8.
50. Khong PL, Leung LH, Chan GC, et al. White matter anisotropy in childhood medulloblastoma survivors: association with neurotoxicity risk factors. Radiology. 2005; 236:647–52.
51. Khong PL, Leung LH, Fung AS, et al. White matter anisotropy in post-treatment childhood cancer survivors: preliminary evidence of association with neurocognitive function. J Clin Oncol. 2006; 24:884–90.
52. Dellani PR, Eder S, Gawehn J, et al. Late structural alterations of cerebral white matter in long-term survivors of childhood leukemia. J Magn Reson Imaging. 2008; 27:1250–5.
53. Nagesh V, Tsien CI, Chenevert TL, et al. Radiation-induced changes in normal-appearing white matter in patients with cerebral tumors: a diffusion tensor imaging study. Int J Radiat Oncol Biol Phys. 2008; 70:1002–10.

54. Welzel T, Niethammer A, Mende U, et al. Diffusion tensor imaging screening of radiation-induced changes in the white matter after prophylactic cranial irradiation of patients with small cell lung cancer: first results of a prospective study. AJNR Am J Neuroradiol. 2008; 29:379–83.
55. Hein PA, Eskey CJ, Dunn JF, et al. Diffusion-weighted imaging in the follow-up of treated high-grade gliomas: tumor recurrence versus radiation injury. AJNR Am J Neuroradiol. 2004; 25:201–9.
56. Sundgren PC, Fan XY, Weybright P, et al. Differentiation of recurrent brain tumor versus radiation injury using diffusion tensor imaging in patients with new contrast enhancing lesions. MRI. 2006; 44:1131–42.
57. Zhou XJ, Leeds NE, Kumar AJ, et al. Differentiation of tumor recurrence from treatment-induced necrosis using quantitative diffusion MRI. Proceedings for the 9th Annual meeting of the International Society of Magnetic Resonance in Medicine. 2001:726.
58. Chenevert T, McKeever P, Ross B. Monitoring early response of experimental brain tumors to therapy using diffusion magnetic resonance imaging. Clin Cancer Res. 1997; 3:1457–1466.
59. Chenevert T, Stegman L, Taylor JM, et al. Diffusion magnetic resonance imaging: an early surrogate marker of therapeutic efficacy in brain tumors. J Natl. Cancer Inst. 2000; 92:2029–2036.
60. Chan YL, Roebuck DJ, Yuen MP, et al. Long-term cerebral metabolite changes on proton magnetic resonance spectroscopy inpatients cured of acute lymphoblastic leukemia with previous intrathecal methotrexate and cranial irradiation prophylaxis. Int J Radiat Oncol. Biol Phys. 2001; 50(3):1, 759–763.
61. Davidson A, Tait DM, Payne GS, et al. Magnetic resonance spectroscopy in the evaluation of neurotoxicity following cranial irradiation for childhood cancer. Br J Radiol. 2000; 73(868):421–424.
62. Chan YL, Yeung DKW, Leung SF, et al. Proton magnetic resonance spectroscopy of late delayed radiation-induced injury of the brain. J Magn Reson Imaging. 1999; 10:130–137.
63. Usenius T, Usenius JP, Tenhunen M, et al. Radiation-induced changes in human brain metabolites as studied by 1H nuclear magnetic resonance spectroscopy in vivo. Int J Radiat Oncol Biol Phys. 1995; 33(3):719–24.
64. Kaminaga T, Shirai K. Radiation-induced brain metabolic changes inthe acute and early delayed phase detected with quantitative proton magnetic resonance spectroscopy. J Computer Assist Tomogr. 2005; 29(3):293–7.
65. Walecki J, Sokól M, Pieniążek P, et al. Role of short Te ^{1}H-MR spectroscopy in monitoring of post-operation irradiated patients. Eur J Radiol. 1999; 30:154–161.
66. Estève F, Rubin C, Grand S, et al. Transient metabolic changes observed with proton MR spectroscopy in normal human brain after radiation therapy. Int J Radiat Oncol Biol Phys. 1998; 40:279–286.
67. Lee MC, Pirzkall A, McKnight TR, et al. ^{1}H-MRS of radiation effects in normal-appearing white matter: Dose-dependence and impact on automated spectral classification. J Magn Reson Imaging. 2004; 19:379–388.
68. PIA JMRI.
69. Weybright P, Sundgren PC, Gomez-Hassan D, et al. Differentiation of Tumor recurrence from treatment related changes using 2D-CSI MR Spectroscopy. AJR. 2005; 185:1471–1476.
70. Rock JP, Hearshen D, Scarpace L, et al. Correlations between magnetic resonance spectroscopy and image-guided histopathology, with special attention to radiation necrosis. Neurosurgery. 2002; 51:912–919.
71. Schlemmer JP, Bachert P, Henze M, et al. Differentiation of radiation necrosis from tumor progression using proton magnetic resonance spectroscopy. Neuroradiology. 2002; 44:216–222.
72. Movsas B, Li BSY, Babb JS, et al. Quantifying radiation therapy-induced brain injury with whole brain proton MR spectroscopy: initial observations. Radiology. 2001; 221:327–331.
73. Isobe T, Matsumura A, Anno I, et al. Changes in 1H-MRSin glioma patients before and after irradiation: the significance of quantitative analysis of choline-containing compounds. No Shinkei Geka. 2003; 31(2):167–72. (abstract in English, article in Japanese).
74. Virta A, Patronas N, Raman R, et al. Spectroscopic imaging of radiation-induced effects in the white matter of glioma patients. J Magn Reson Imaging. 2000; 18:851–857.

75. Atwood T, Robbins ME, Zhu J-M. Quantitative in vivo proton MR spectroscopic evaluation of the irradiated rat brain. J Magn Reson Imaging. 2007; 26(6):1590–1596.
76. Atwood T, Payne VS, Zhao W, et al. Quantitative magnetic resonance spectroscopy reveals a potential relationship between radiation-induced changes in rat brain metabolites and cognitive impairment. Radiat Res. 2007; 168(5):574–81.
77. Chong VF, Rumpel H, Fan YF, et al. Temporal lobe changes following radiation therapy: Imaging and proton MR spectroscopic findings. Eur Radiol. 2001; 11:317–24.
78. Chong VF, Rumpel H, Aw YS, et al. Temporal lobe necrosis following radiation therapy for nasopharyngeal carcinoma: 1H MR spectroscopic findings. Int J Radiat Oncol Biol Phys. 1999; 45:699–705.
79. Schlemmer HP, Bachert P, Herfarth K, et al. Proton MR spectroscopic evaluation of suspicious brain lesions after stereotactic radiotherapy. ANJR Am J Neuroradiol. 2001; 22:1316–24.
80. Castillo M, Kwock L, Mukherji SK. Clinical applications of proton MR spectroscopy. AJNR Am J Neuroradiol. 1996; 17:1–15.
81. Yeung DK, Chan Y, Leung S, et al. Detection of an intense resonance at 2.4 ppm in 1H MR spectra of patients with severe late-delayed, radiation-induced brain injuries. Magn Reson Med. 2001; 45:994–1000.
82. Zeng QS, Li CF, Zhang K, et al. Multivoxel 3D proton MR spectroscopy in the distinction of recurrent glioma from radiation injury. J Neurooncol. 2007; 84:63–9.
83. Kimura T, Sako K, Gotoh T, et al. In vivo single voxel proton MR spectroscopy in brain lesions with ring-like enhancement. NMR Biomed. 2001; 14:339–49.
84. Rock JP, Scarpace L, Hearshen D, et al. Associations among magnetic resonance spectroscopy, apparent diffusion coefficients and image-guided histopathology with special attention to radiation necrosis. Neurosurgery. 2004; 54:1111–9.
85. Di Chiro G, Oldfield E, Wright DC. Cerebral necrosis after radiotherapy and/or intraarterial chemotherapy for brain tumors. PET and neuropathologic studies. AJR. 1988; 150:189–97.
86. Langleben DD, Segall GM. PET in differentiation of recurrent brain tumor from radiation injury. J Nucl Med. 2000; 41:1861–7.
87. Thompson TP, Lunsford LD, Kondziolka D. Distinguishing recurrent tumor and radiation necrosis with positron emission tomography versus stereotactic biopsy. Stereotact Funct Neurosurg. 1999; 73:9–14.
88. Matheja P, Rickert C, Weckesser M, et al. Scintigraphic pitfall: delayed radionecrosis. Case illustration. J Neurosurg. 2000; 92:732.
89. Hahn CA, Zhou SM, Raynor R, et al. Dose-dependent effects of radiation therapy on cerebral blood flow, metabolism, and neurocognitive dysfunction. Int. J. Radiation Oncology Biol.Phys. 2009; 73(4):1082–1087.
90. Katoh N, Nakada K, Takei T, et al. Methionine PET in differentiating recurrent brain tumor from radiation necrosis following cranial radiation. International Congress Series. 2004; 1264:217–221.
91. Lee MC, Cha S, Chang SM, et al. Dynamic susceptibility contrast perfusion imaging of radiation effects in normal-appearing brain tissue: changes in the first-pass and recirculation phases. J. Magn Reson Imaging. 2005; 21(6):683–93.
92. Cao Y, Tsien CI, Sundgren P, et al. DCE MRI as a Biomarker for Prediction of Radiation-Induced Neurocognitive Dysfunction. Clinical Cancer Research. 2009 (in press).
93. Taki S, Higashi K, Oguchi M, et al. Changes in regional cerebral blood flow in irradiated regions and normal brain after stereotactic radiosurgery. Annul Nucl. Med. 2002; 16(4):273–7.
94. Jain R, Scarpace L, Ellika S, et al. First-pass perfusion computed tomography: initial experience in differentiating recurrent brain tumors from radiation effects and radiation necrosis. Neurosurgery. 2007; 61:778–86.

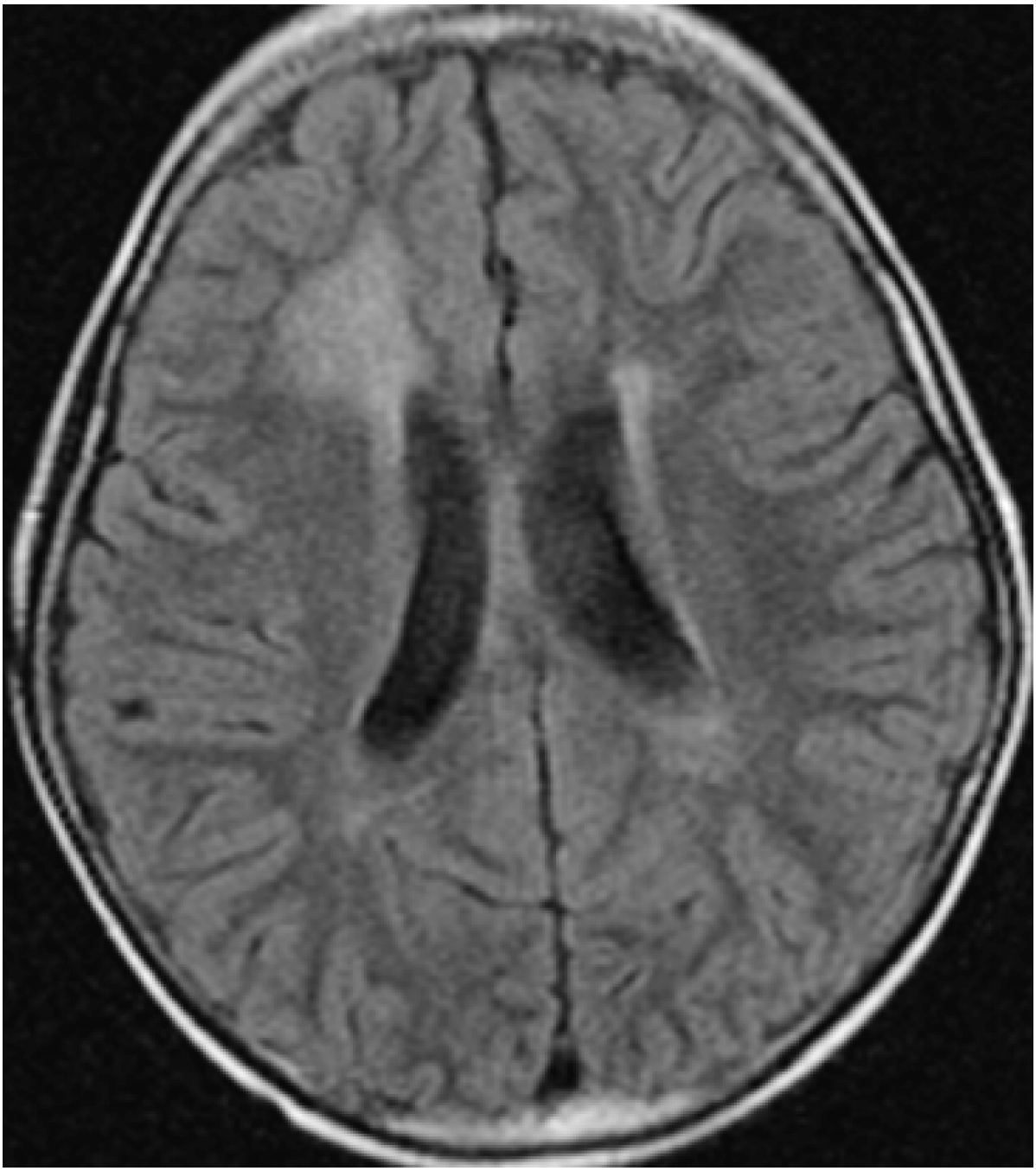

Figure 1.
Axial Fluid Attenuation Inversion Recovery (FLAIR) image demonstrate the increased signal in predominately right frontal lobe in a patient with radiation injury sceondary to irradaition.

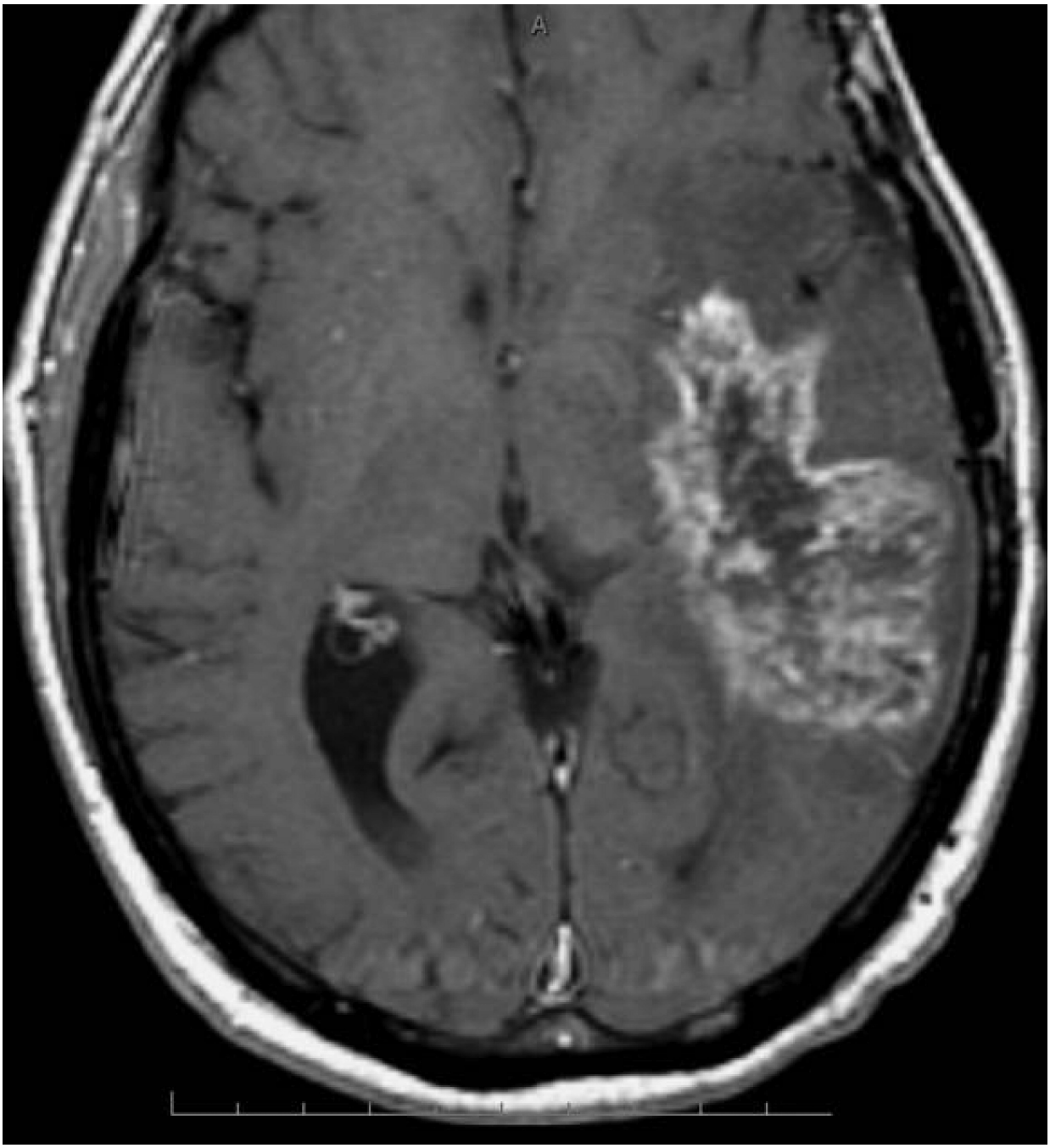

Figure 2.
Axial post GD-DTPA T1-weighted image of Swiss-cheese appearance of contrast enhancement in a case of surgically proven radiation necrosis.

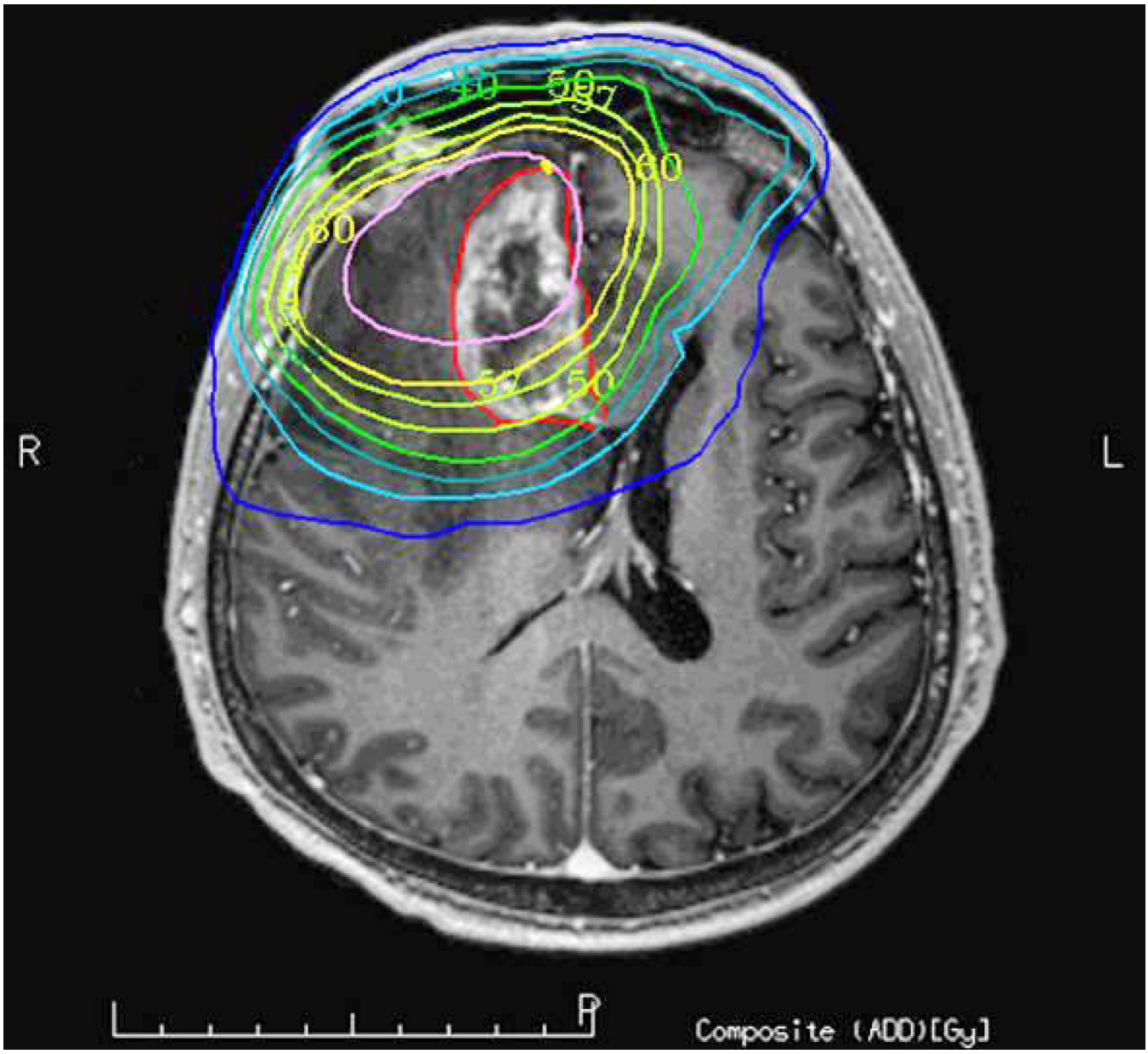

Figure 3 a-b.

Axial post Gd-DTPA T1-weighted image demonstrates a focal heterogeneously enhancing lesion in the right frontal lobe. The lesion that was histopahtology proven radiation necrosis is outlined in red (a). The lesions is in so-called in-field of the radiation dosage volume but only parts of the lesion is in the high 60Gy field while other parts are outside the high dose (b).

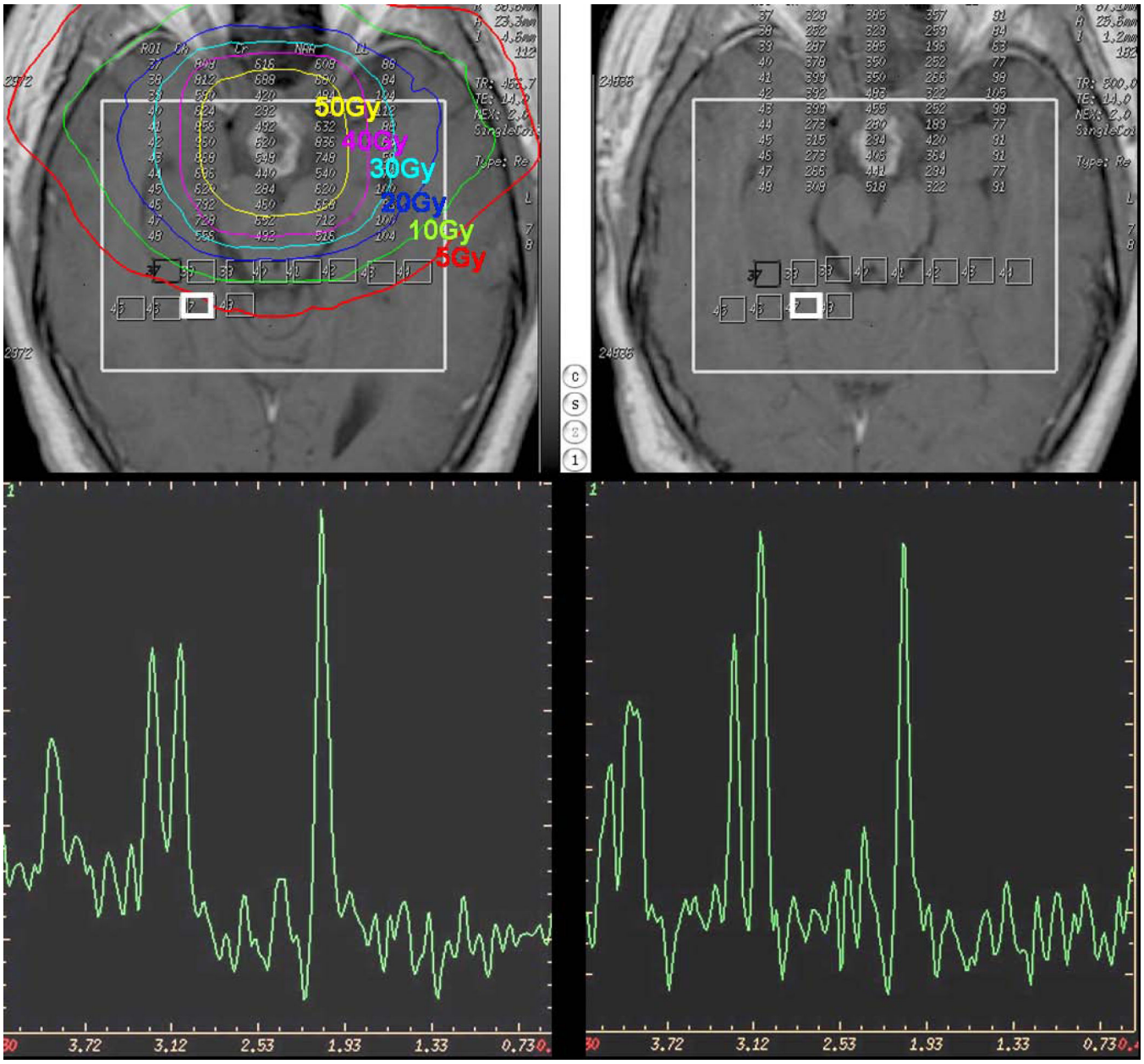

Figure 4 a-d.

Post Gd-DTPA T1-weighted images prior to RT (top left) and 6 months after the completion of RT (top right). The large white boxes represent the VOIs for MRS acquisition, and small white boxes depict the individual VOIs for spectral analysis. The two representative spectra prior to radiation treatment (bottom left) and 6 months after radiation treatment (bottom right) were from the corresponding bright white boxes in top panels. Color contours denote isodose lines of radiation.

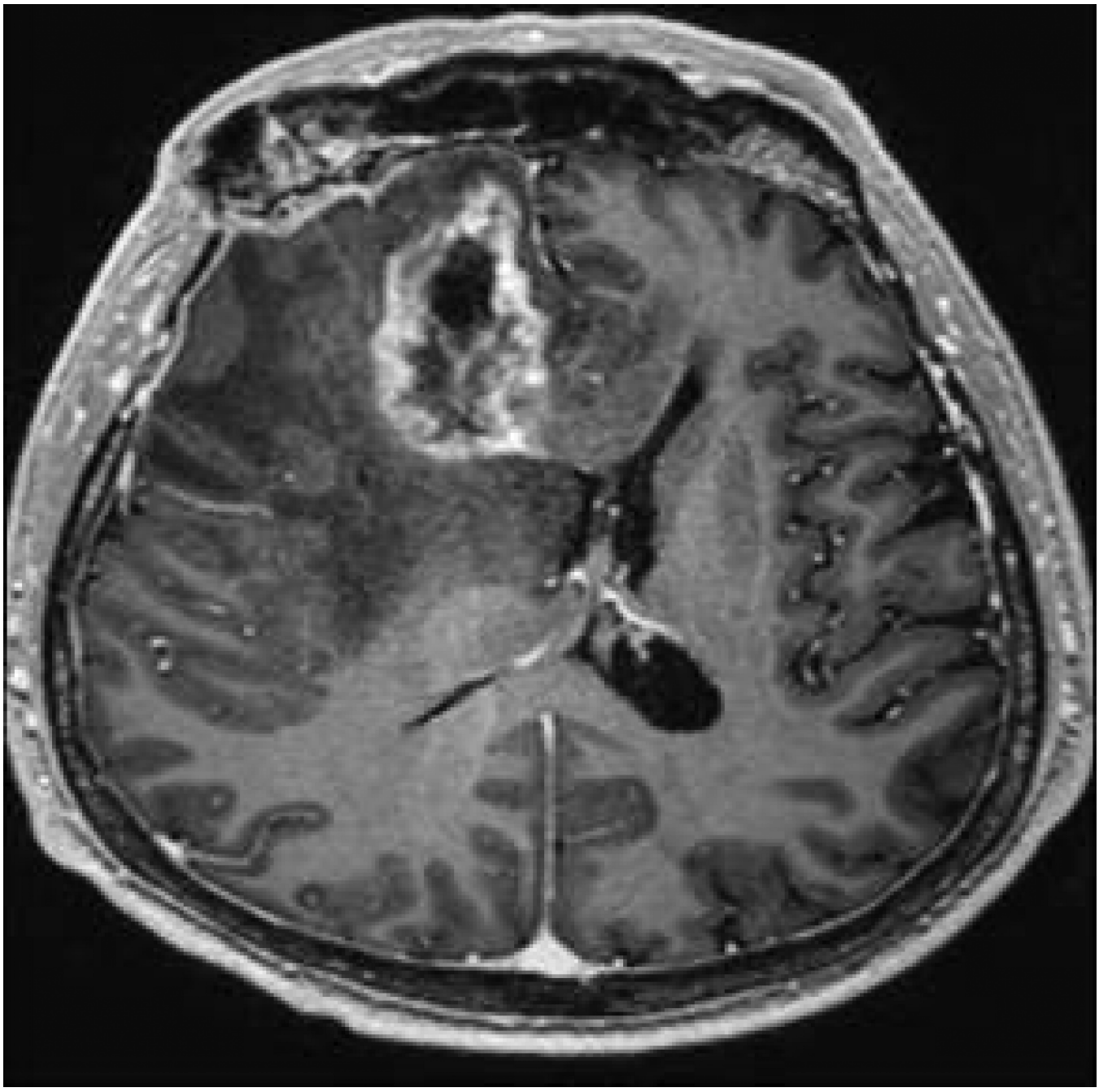

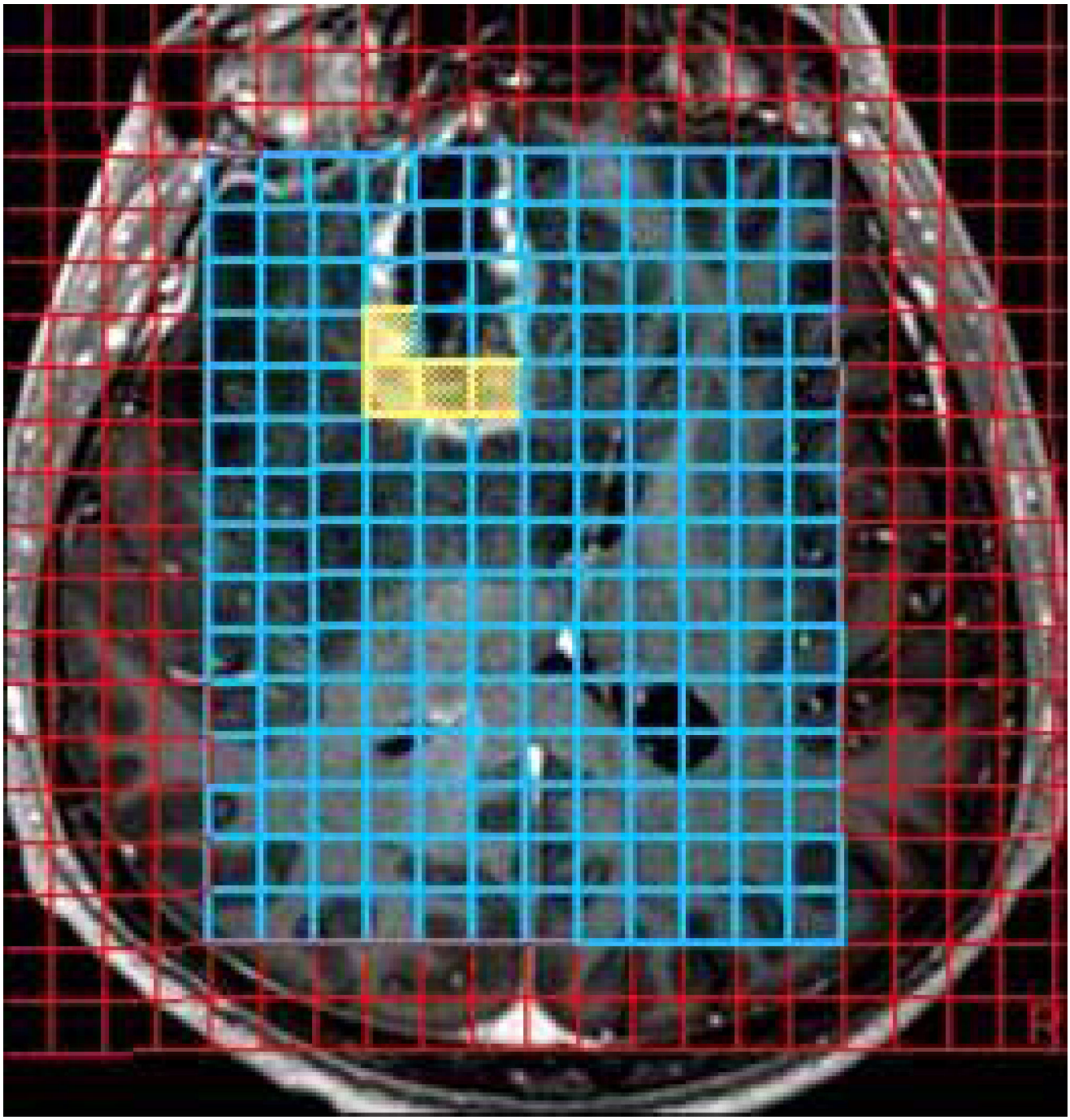

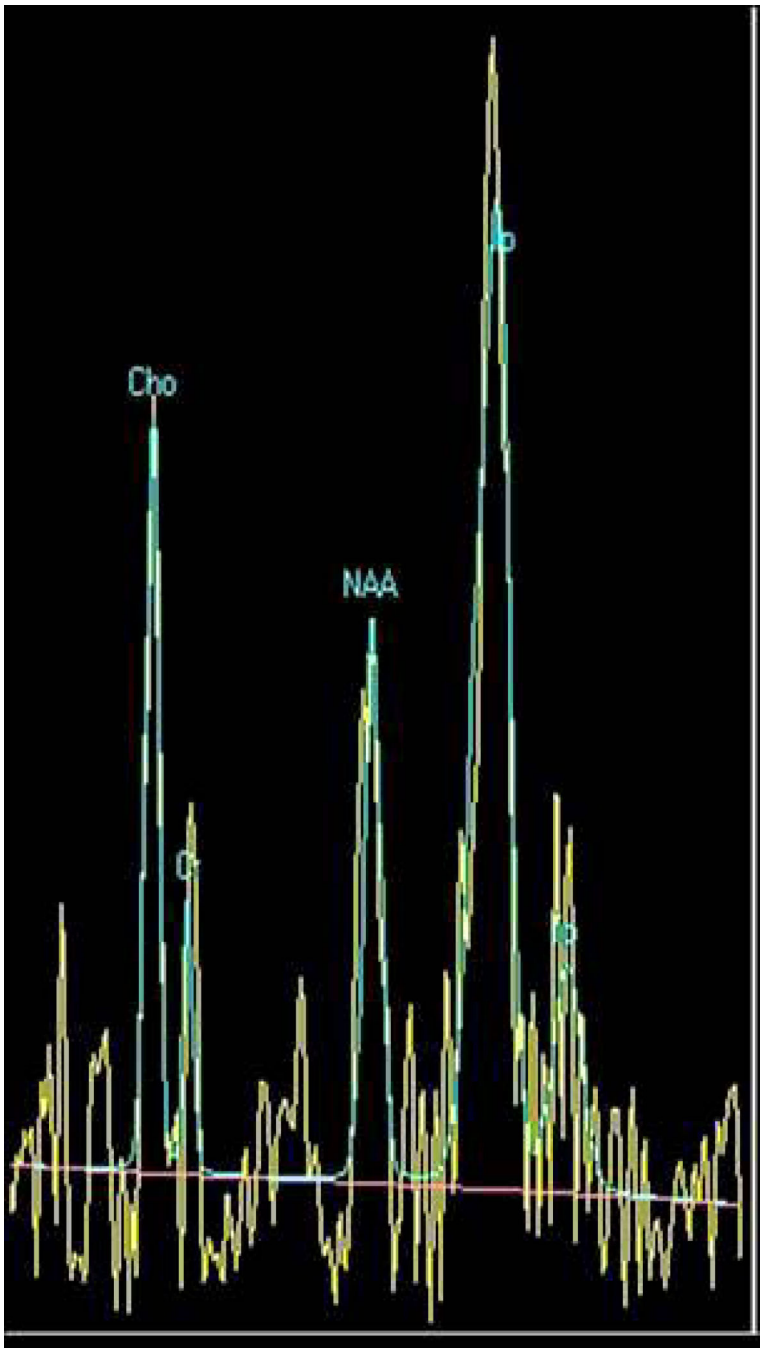

Figure 5 a-c.

Axial post GD-DTPA T1-weighted image demonstrates a focal heterogeneously enhancing lesion in the right frontal lobe. The volume of interest (VOI) of the 3D-CSI (chemical shift imaging) MR spectroscopy (b) and corresponding spectra with significantly elevated lipid peak, slight decrease in NAA peak and slight increase in the choline peak. The lesion was surgically removed and was proven to be radiation necrosis.